fibers

MDPI

Article

Production of Decolorized Mushroom Pulp for Nonwoven Cotton Composite

Ho-Seong Im [1], Satomi Tagawa [2], Jae-Seok Jeong [3] and Hyun-Jae Shin [1,*]

[1] Department of Chemical Engineering, Graduate School, Chosun University, 309 Pilmun-daero, Dong-gu, Gwangju 61452, Republic of Korea; ghtjd0731@naver.com
[2] Faculty of Engineering, University of Miyazaki, 1-1 Gakuen Kibanadai-Nishi, Miyazaki 889-2192, Japan; tagawa.satomi.c0@cc.miyazaki-u.ac.jp
[3] Korea Textile Development Institute (KTDI), 136 Gukchaebosangro (Jungri-dong), Seo-gu, Daegu 41842, Republic of Korea; jsh6022@textile.or.kr
* Correspondence: shinhj@chosun.ac.kr; Tel.: +82-62-230-7518

Highlights

What are the main findings?

- Sustainable Cotton Alternative: Decolorized mushroom pulp (DMP) was developed as an eco-friendly substitute for cotton, with hydrogen peroxide (H_2O_2) being the most effective decolorization agent for fruiting bodies.
- Non-woven Textile Fabrication: DMP was successfully combined with cotton fibers to create non-woven textiles, highlighting its potential for sustainable fabric production.

What are the implications of the main findings?

- Environmental Impact: Using DMP as a cotton alternative can reduce water consumption, pesticide use, and soil degradation in the textile industry.
- Industrial Application: The successful integration of DMP into non-woven fabrics suggests its potential for use in the commercial-scale production of sustainable textiles.

Abstract: Cotton, widely used in the textile industry, has a significant environmental impact due to soil degradation and excessive water consumption during cultivation. As a result, there is a growing need for biodegradable alternatives. This study pioneers the development of decolorized mushroom pulps (DMPs) from edible mushrooms as a sustainable replacement for cotton. Decolorization of fruiting bodies showed the highest reactivity with hydrogen peroxide (H_2O_2). At the same time, mycelium responded more effectively to sodium hypochlorite (NaClO), though this led to structural changes such as melting and twisting. Potassium was detected in fruiting bodies but absent in mycelium, and higher salt content was noted in *Agaricus bisporus* and *Trametes orientalis* compared to *Pleurotus ostreatus* and *Flammulina velutipes*. Future research should focus on preserving mycelial integrity or developing strains that eliminate the need for decolorization treatments, advancing DMPs as viable biotextile materials.

Keywords: biotextile; decolorization; edible mushrooms; mycelium; mushroom pulp; nonwoven composite

check for updates

Academic Editor: Martin J. D. Clift

Received: 26 December 2024
Revised: 23 January 2025
Accepted: 26 February 2025
Published: 5 March 2025

Citation: Im, H.-S.; Tagawa, S.; Jeong, J.-S.; Shin, H.-J. Production of Decolorized Mushroom Pulp for Nonwoven Cotton Composite. *Fibers* **2025**, *13*, 30. https://doi.org/10.3390/fib13030030

Copyright: © 2025 by the authors. Licensee MDPI, Basel, Switzerland. This article is an open access article distributed under the terms and conditions of the Creative Commons Attribution (CC BY) license (https://creativecommons.org/licenses/by/4.0/).

1. Introduction

The Earth is experiencing characteristic global warming by 2023 due to environmental pollution caused by industrialization [1]. Among them, petrochemical materials, the livestock industry, and food/clothing crop cultivation are representative sources of pollution.

In the case of clothing crops, cotton cultivation has a significant environmental impact [2]. Cotton is a water-intensive crop requiring large amounts of irrigation. It can take over 20,000 L of water to produce just 1 kg of cotton [3]. Conventional cotton farming practices often lead to soil erosion and degradation. Monoculture of cotton for extended periods depletes soil nutrients and quality [4]. Next, cotton farming heavily relies on pesticides and fertilizers. These chemicals contaminate soil and water sources, harming ecosystems and biodiversity [2,5]. The cotton industry contributes to climate change through greenhouse gas emissions from synthetic fertilizer use and carbon dioxide emission, estimated at approximately 5% of global greenhouse gas emissions [6]. Therefore, it is necessary to develop materials to replace cotton consumed in multiple fields, such as medical, clothing, paper, and packaging.

Mushrooms are used in various fields, such as packaging materials, alternative leather, and alternative meat, to solve multiple environmental pollution [7–10]. They are considered one of the means to replace cotton. They are fungi that grow on lignocellulosic substrates—mainly oak—and can be broadly categorized into two parts. The fruiting body is where the individual forms reproduce, and the mycelium is where the individual forms to absorb nutrients [11,12]. They are composed of single-stranded fibrous hyphae and possess three types of hyphae (generative, skeletal, and binding), depending on the strain [13]. In addition, they have a cell wall on the surface, the main components of which are chitin, glucans ((1,3)-α-glucan, (1,3)-β-glucan, (1,4)-β-glucan, (1,6)-β-glucan), mannoprotein (glycoprotein), and pigments [14,15]. Pigments are present in various forms, including carotenoids and melanin, depending on the strain, and play multiple roles, such as free radical scavenging, of which melanin has been reported in various mushroom species such as *Pleurotus* spp. and *Trametes* sp. [15–17].

Life cycle assessment (LCA) studies of mushroom-based materials (MBMs), which have recently gained attention as an eco-friendly material, have been conducted and reported to have environmental benefits compared to conventional materials such as plastics and concrete [18–20]. These materials, mainly made from mushroom mycelium and agricultural by-products, have been reported to reduce carbon emissions by up to 55% and water consumption by 44% during production compared to fossil-based materials [19,20]. They are also biodegradable and can be composted when disposed of, helping to achieve circular economy goals.

Biotextiles refer to textiles produced from bioresources such as fungi (e.g., mushrooms) or bacterial cellulose, and they are increasingly researched as potential alternatives to conventional polymer-based materials [21,22]. In the production of textiles, naturally occurring pigments present in bio-based materials can impact the esthetic and functional qualities of the final product. These pigments may compromise product consistency, particularly in color uniformity, if not adequately managed. Therefore, it is essential to employ physicochemical treatments to remove these pigments or suppress their activity with de-colorants to maintain product quality. Decolorants are generally categorized into oxidative and reductive types [23]. However, among the reductive decolorants, sulfur compounds were excluded from this study due to the environmental concerns associated with their use.

Nakauchi et al. proposed mushrooms as a possible source of this pulp [24]. The following directions were investigated in the present study to differentiate from the above studies. First, mushroom pulp was used to make cotton composites by incorporating it into non-woven fabrics that did not exist before. Next, we proposed a method that can be used to diversify the decolorant used in the production of mushroom pulp. In addition, we produced various sizes from micro-scale pulp to macro-scale pulp. We did not use the

homogenization method, and we expanded the range of materials by using mushroom fruiting bodies and mycelium.

2. Materials and Methods

2.1. Materials

Sodium hydroxide (NaOH), hydrogen peroxide (H_2O_2), sodium oxalate ($Na_2C_2O_4$), sodium hypochlorite (NaClO), Bacto™ yeast extract, Bacto™ malt extract, Bacto™ peptone, Bacto™ agar, and Difco™ potato dextrose agar (PDA; potato starch 4 g/L, dextrose 20 g/L, agar 1.5 g/L) were purchased from Duksan Pure Chemical Co., Ltd., Ansan, Republic of Korea, and used in the experiments. The distilled water used throughout the experiments was produced using a manufacturing device (C-DIS1, Changsin, Seoul, Republic of Korea). A fluorescent staining reagent for DMPs, Calcofluor white M2R (CFW) was purchased from Sigma-Aldrich Corp. (Tokyo, Japan). Finally, the cotton fiber used in the production of the textile composite was supplied by Meriqueen Co., Ltd., Namyangju, Republic of Korea. Initially, in a randomly arranged state, the fibers were aligned in a unidirectional orientation using a gilling machine (Hansin Wool Textile Co., Ltd., Busan, Republic of Korea) and then cut into 5 to 7 mm lengths for use.

2.2. Strain

The fruiting bodies (*Agaricus bisporus*, *Flammulina velutipes*, and *Pleurotus ostreatus*) used in the experiment were purchased from a local market. They cut them into 5 and 10 mm long slices (Table 1). The fruiting body strains used in this study were selected from the highest-yielding mushrooms cultivated in Korea from 2005 to 2022 [25]. The strains used as mycelium were pre-evaluated for their ability to produce mycelial mats and excellent culture characteristics (e.g., growth rate, mycelial density, and culture stability) [26]. This choice was because these mushrooms can be produced reliably and in large quantities in Korea and are an economical and sustainable source of raw materials. To obtain the mycelium for further use, strains were isolated from these fruiting bodies, cultured on sterile PDA media, stored at 4 °C in a full plate growth state, and assigned a code number corresponding to each strain's abbreviations. The mycelium of *Trametes orientalis* used in the study was derived from the JF-82 strain obtained from the Jeollanam-do Forest Research Institute (Naju-si, Jeollanam-do, Republic of Korea). To promote rapid growth and the formation of a mycelial mat, a mutant strain was utilized, which had undergone gamma-ray irradiation (200 Gy) using a Cobalt-60 source Gamma-ray irradiator (MDS Nordion, Ottawa, ON, Canada) available at the Korea Atomic Energy Research Institute (KAERI; Jeongup-si, Jeollabuk-do, Republic of Korea). The mycelial mat was cultivated following the methodology described in the study by Jeong et al. [27]. Specifically, the mycelium isolated from the fruiting bodies was inoculated onto modified YM agar medium (yeast extract; 3 g/L, malt extract; 3 g/L, peptone; 5 g/L, dextrose; 10 g/L, agar; 15 g/L) and subculture three times to maximize its viability before undergoing gamma-ray treatment at the KAERI facility. The irradiated strains were validated for mutations through confrontation culture with non-irradiated strains. When a zone was formed between the interfaces, part of the mutant mycelium was isolated, cultured on fresh PDA, and then inoculated into a substrate prepared with oak sawdust and rice bran mixed at an 8:2 volume ratio, with a moisture content of 55–60%. The substrate was sterilized in an autoclave at 121 °C for 60 min, cooled to room temperature, and inoculated with liquid inoculum. The mycelial mat formed after 30 days of incubation was harvested, washed, and used in the experiment.

Table 1. Fungal strains used in this study.

Fungal Species	Abbreviation	Type	Structure
Agaricus bisporus Hongo	CSU *-AB	Fruiting body	Monomitic
Pleurotus ostreatus (Jacq.) P. Kumm.	CSU-FV		
Flammulina velutipes (Curtis) Singer	CSU-PO		Dimitic
Trametes orientalis (Yasuda) Imazeki	CSU-ToM	Mycelial mat	Trimitic

* Abbreviation of Chosun University.

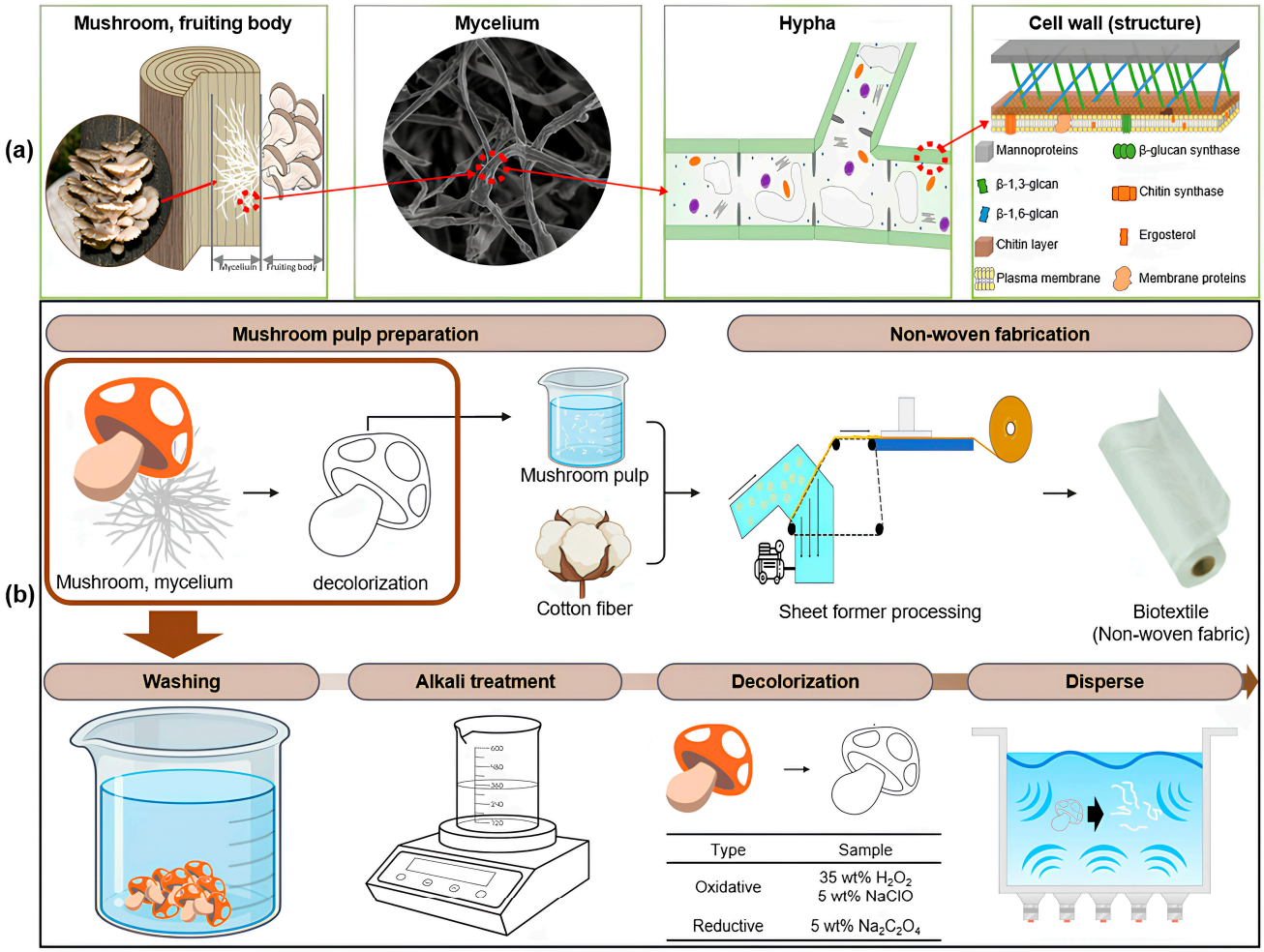
2.3. DMP Manufacturing

The DMP production process was modified based on the mycelium pulp preparation method described by Nakauchi et al. and is outlined in Scheme 1 [24]. The prepared fruiting bodies and mycelial mat were cut into 5 to 8 mm lengths and soaked in distilled water for 30 min to remove any substances attached during cultivation and distribution. This initial washing step was followed by a pretreatment process using a 5 wt% NaOH solution at a volume ratio of 10:1 relative to the sample, where the samples were treated for 60 min. The purpose of this NaOH treatment was to enhance bleaching efficiency by causing slight surface damage to the mycelium and increasing the distance between mycelial structures, which facilitates the penetration of bleaching agents. After pretreatment, the samples underwent oxidative decolorizing, including 35 wt% H_2O_2 and 5% NaClO solution, and a reductive decolorant, 5% $Na_2C_2O_4$ solution. The samples were then subjected to sonication for 3 min, stirring at 25 °C to ensure a thorough mixing and reaction. During this process, the ratio of decolorant to sample was maintained at a volume ratio of 5:1 to produce the mushroom pulp. The pulp was then thoroughly washed and neutralized using a 30-µm pore size testing sieve (Nonaka Rikaki Co., Ltd., Tokyo, Japan) and distilled water to remove residual chemicals and stabilize the pulp. Finally, the DMP retained on the sieve was adjusted to a 10 wt% pulp content by adding distilled water, followed by moisture analysis using a moisture analyzer (MA 100, Sartorius, Gottingen, Germany). The prepared DMPs were stored at 4 °C until use.

2.4. Nonwoven Composite Fabrication

The DMPs were processed following a modified version of the nonwoven fabric manufacturing procedure as referenced by Yoon et al. [28]. The process was conducted using Beater (Niagara beater No. 2505, Kumagai Riki Kogyo Co., Ltd., Tokyo, Japan), Semi-auto type Sheet former (Sheet former, Frank-Pti, Birkenau, Germany), and Rotary dryer (Calendaring; DR-200, Kumagai Riki Kogyo Co., Ltd., Tokyo, Japan), which are facilities housed at the Korea Institute of Industrial Technology (KITECH; Ansan-si, Gyeonggi-do, Republic of Korea) and Korea Textile Development Institute (KTDI; Dalseo-gu, Daegu, Republic of Korea). At KITECH, pure DMPs produced nonwovens, while cotton and DMP composite textiles were produced at KTDI. The DMP strains used in the composite production were *P. ostreatus* and *F. velutipes*. The detailed sheet-forming process for nonwoven materials involved several stages. The DMP dispersion was initially prepared using a beater equipped with a circulating tank and toothed gear. The process alternated between two stages: the beating stage, where the gear physically impacted the pulp to achieve dispersion, and the releasing stage, where the gear was retracted to facilitate smooth water circulation within the tank. This cycle of dispersion (20 s) and releasing (10 s) was repeated continuously for 3 min. In the sheet-forming step, the DMP solution was separated. Once the dispersion was introduced into the machine and water-filled internal tank, the air was injected to create a bubbling effect to help disentangle fibers. A couching process was subsequently applied, during which a pressure of 3 bar was used to flatten the fibers and reduce moisture.

Finally, the calendaring process was carried out using a rotary dryer set to 121 °C to remove residual moisture and complete the fabrication process.



Scheme 1. (**a**) Basic classification of mushroom structure; (**b**) Decolorized mushroom pulp (DMP) and fabrication process (this scheme was created using Microsoft Office Professional Plus 2019 with bioRender image library (Toronto, ON, Canada)).

2.5. Analysis

2.5.1. Morphology

An ultra-high-resolution Field-emission Scanning Electron Microscope (FE-SEM; SU-8600, Hitachi, Tokyo, Japan) was used to evaluate the surface changes at each stage of DMP production. Initially, a 10% DMP solution was stored in an ultra-low temperature freezer at −80 °C for 8 h, followed by lyophilization using a freeze-dryer (MLB-9003, Mareuda, Gwangju, Republic of Korea) for 24 h. This process is essential for preserving the structural integrity of the samples during observation. A 0.01 g portion of the dried sample was placed on a rubber-based double-sided tape affixed to a specimen observation plate. The sample was coated with gold using an ion sputter coater (G20, GSEM, Suwon, Republic of Korea) for approximately 20 min to facilitate clear surface observation under the electron microscope. The surface observation was conducted under a vacuum with an acceleration voltage of 15 kV.

Furthermore, an energy-dispersive X-ray (EDX) microanalyzer attached to the FE-SEM was used to complement the surface imaging to analyze the atomic composition and content within the observed area after magnifying the sample 300 times. This analysis

provided detailed insights into the elemental distribution correlating with the observed surface morphology.

2.5.2. Confocal Laser Scanning Microscopy (CLSM)

To observe the microstructure of the DMP nonwoven fabric, fluorescence imaging was performed using a confocal laser scanning microscope. The fungal hyphae cell walls were stained with CFW, and fluorescence was detected at an excitation wavelength of 405 nm and an emission wavelength of 410–500 nm. A z-stack was performed with a step size of 5.4 μm, and a single focused image was obtained by integrating the acquired optical section images.

2.5.3. Fourier-Transform Infrared (FT-IR)

To investigate the impact of physicochemical treatments on the functional groups of DMPs, FT-IR (FT-IR Spectrometer, Thermo Scientific, Waltham, MA, USA) was employed. The measurements were conducted in the Attenuated Total Reflectance FT-IR (ATR-FTIR) mode using a diamond crystal ATR accessory, which is ideal for analyzing surface properties. The samples were freeze-dried and then pressed into a flat form to ensure uniform surface conditions, a critical factor for obtaining reliable and consistent spectra. The spectral analysis was performed over a range of 650 to 4400 cm^{-1} using the built-in software, allowing for a detailed observation of changes in functional groups.

2.5.4. X-Ray Diffractometer (XRD)

To investigate the impact of physicochemical treatments on the crystalline structure of components such as chitin and glucans in the mycelial cell wall, an X-ray Diffractometer (XRD; Multipurpose X-ray diffractometer, Malvern Panalytical, Malvern, UK) was utilized. The DMP samples were re-grounded and then pressed into a flat form to ensure a uniform surface for accurate measurement. The diffraction angle of 2 theta was measured from 3° to 40° with a scanning rate of 2°/min and a step size of 0.02°. The results were analyzed using software (X'pert HighScore software (ver. 5.1), Malvern Panalytical, Malvern, UK) to identify specific changes in the crystalline structure.

2.5.5. Color Parameter

A colorimeter (Colorimeter Pro, CHNSPEC, Hangzhou, China) was used to analyze the color parameters to quantitatively evaluate the effectiveness of the bleaching treatment on the fruiting bodies and mycelial mats. The white standard provided with the instrument was used to set the reference point (L* = 94:0.4:0.7). The International Commission on Illumi-nation-L*, a*, b* (CIELAB) parameters were measured using this device and then converted to RGB for visual comparison. The ranges for L*, a*, and b* were 0 (black) to 100 (white), −128 (green) to 128 (red), and −128 (blue) to 128 (yellow), respectively, with the RGB values ranging from 0 (black) to 255 (colors) for all three parameters, allowing for a comprehensive assessment of the decolorization effects. The statistical analyses were performed using R software (ver. 4.4.2) within the R studio environment. Both one-way analysis of variance (ANOVA) and the Tukey HSD test were performed simultaneously, and *p*-values were calculated to determine the significance levels. The confidence level was set at 95%. Data were measured in 10 replicates for each sample to ensure statistical reliability.

3. Results and Discussion

3.1. DMP Morphology and Elemental Contents

DMPs were dispersed by sonication in distilled water, resulting in a highly viscous and well-dispersed solution. This process was essential to ensure uniformity before conducting

further analyses. The morphology of the DMPs, examined using SEM on freeze-dried samples, provided crucial insights into the changes induced by physicochemical treatments. Figure 1a–d show that the surface analysis of non-treated DMPs revealed significant morphological features. In the SEM image of *P. ostreatus*, a spherical object of 25–30 µm on the right side was identified as a basidiospore, located initially within the gills (also known as lamellae) under the mushroom cap [29]. This observation is consistent with previous research, showing the formation of a three-dimensional porous network. In contrast, *F. velutipes* displayed a unidirectional mycelial growth structure, which its unique fruiting body formation can explain. Unlike *P. ostreatus* and *A. bisporus*, which form thick fruiting bodies, *F. velutipes* appear to develop a thin and elongated fruiting body, resulting in predominantly unidirectional mycelial growth. Figure 1e–h show the SEM images of *P. ostreatus* after each stage of treatment. Following NaOH treatment, the distance between hyphae increased, likely due to the hydrogen bonds formed between the hydroxyl groups of various cell wall components (polysaccharides, proteins, etc.), which allowed water to penetrate between the hyphae [30]. After decolorization, the samples exhibited partial deformation (cut, melt, twist) due to the chemical treatments. This damage is attributed to the increased distance between hyphae and the softening of the cell walls caused by the pretreatment, which facilitated the action of the decolorants. This pattern was observed consistently across all four strains; however, *A. bisporus* and *T. orientalis* displayed some unique phenomena. In the case of *A. bisporus* (Figure 1i), deformation (melting) was observed as early as the NaOH treatment, unlike the other strains. This is likely due to the thinner hyphae of *A. bisporus* (monomitic) compared to *F. velutipes* (dimitic) and *T. orientalis* (trimitic), making it more susceptible to cell wall damage from NaOH treatment. However, the fact that *P. ostreatus*, despite being monomitic, did not show similar damage under the same conditions suggests that further studies, such as measuring hyphal thickness or cell wall components are necessary to understand this discrepancy [30]. As seen in Figure 1j, salt formations due to NaClO treatment were observed on the SEM, which is consistent with the findings of Nawaz et al. [31]. During pretreatment, some chitin in the cell walls likely reacted with NaOH, partially converting to chitosan through nucleophilic acyl substitution [32]. The NaClO decolorization process likely resulted in the substitution of the primary amine at the C-2 position of the chitosan pyranoid structure with an N-halamine, similar to the observations made in this study. Gómez-Salazar et al. (2021) analyzed how the sonication of food materials affects salt reduction. They reported that in the case of cooked ham, sonication resulted in a 32% reduction in salt concentration compared to conventional methods, causing an effective reduction while maintaining product quality [33]. These studies suggest that ultrasonic treatment of salt retained in the pulp can increase the salt penetration and diffusion rate and effectively remove salt without physical damage. In addition, because it is a physical cleaning method, the amount of chemicals used for cleaning can be reduced to minimize surface damage. However, due to the high energy consumption of ultrasonic equipment, the economics must be carefully considered.

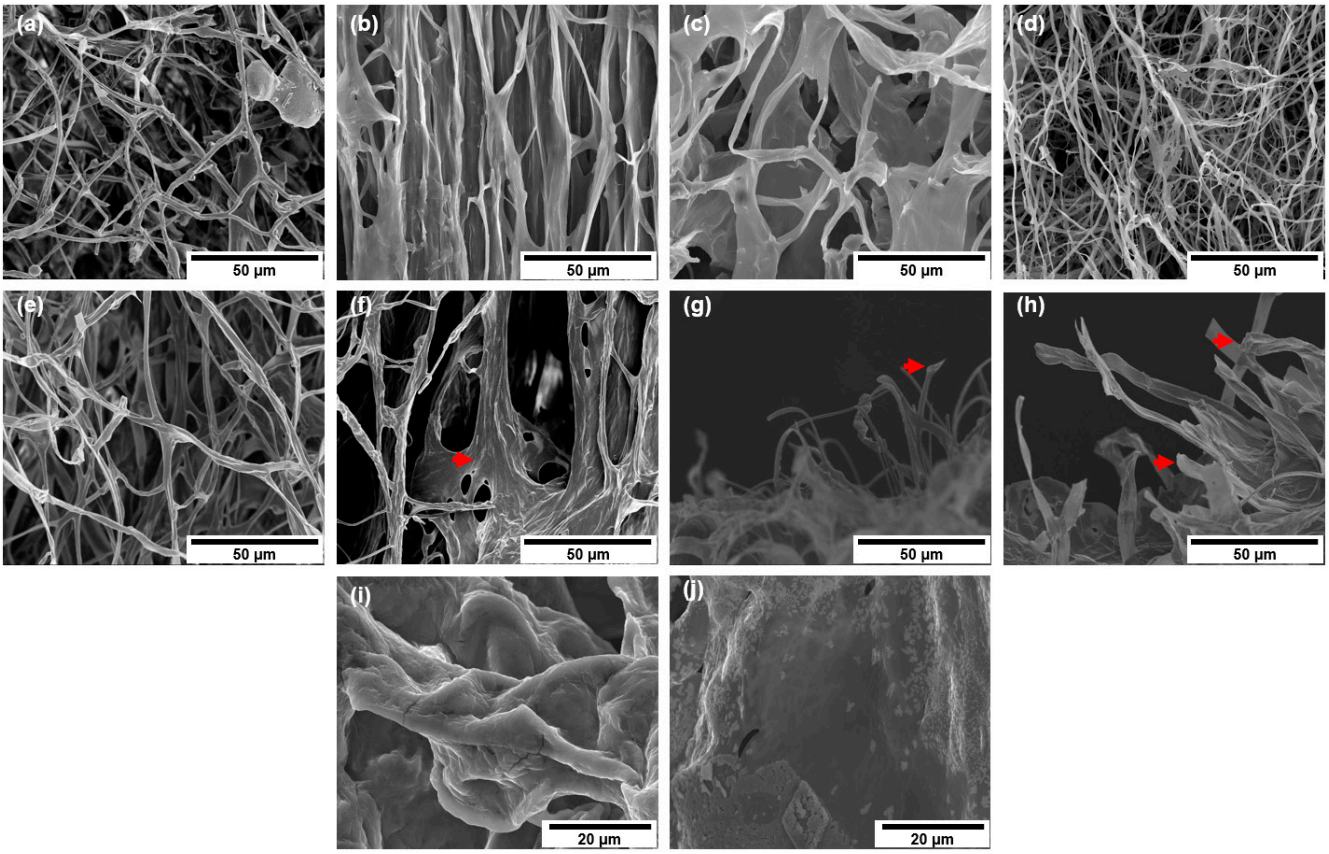


Figure 1. SEM images of mushroom strains ((**a**–**h**) magnification ×1000, scale bar = 50 µm, (**i**,**j**) magnification ×2000, scale bar = 20 µm, red arrows: mycelial deformation due to chemical decolorization; melt, cut, and twist): (**a**) non treated *Pleurotus ostreatus*; (**b**) non treated *Flammulinva velutipes*; (**c**) non treated *Agaricus bisporus*; (**d**) non treated *Trametes orientalis*; (**e**) 5 wt% NaOH treated *P. ostreatus*; (**f**) 5 wt% NaOH and 35 wt% H_2O_2 decolorized *P. ostreatus*; (**g**) 5 wt% NaOH and 5 wt% NaClO decolorized *P. ostreatus*; (**h**) 5 wt% NaOH and 5 wt% $Na_2C_2O_4$ decolorized *P. ostreatus*; (**i**) 5 wt% NaOH treated *A. bisporus* and (**j**) 5 wt% NaOH and 5 wt% NaClO decolorized *A. bisporus*.

3.2. FT-IR

Next, ATR-FTIR spectra were obtained to assess the impact of physicochemical treatments on the chemical composition of hyphal fibers (Table 2). The spectra of all untreated strains were found to be similar, with characteristic peaks corresponding to polysaccharides (chitin, glucans; 1372–910 cm^{-1}), proteins (1650–1535 cm^{-1}), lipids (2996−2800 cm^{-1}), and phosphate compounds (1407−1150 cm^{-1}) [24], all of which are integral components of the hyphal cell wall, as shown in Figure 2. The strong and overlapping bands in the 1150–900 cm^{-1} region, primarily associated with C–C and C–O stretching vibrations in pyranosides, indicate polysaccharides, commonly called the "sugar region" [34–36]. A distinct band around 1035 cm^{-1} was consistently observed across all DMPs, corresponding to pyranoside bonds' C–O–C stretching vibration [37]. This region, which includes bands at 1372, 1322, 1250, 1200, 1150, 1076–1071, 1040–1033 cm^{-1}, as well as 1020 cm^{-1}, reflects the presence of a mixture of hyphal cell wall polysaccharides, including α-glucan, branched (1–3)(1–6)-β-D-glucan, linear (1–3)-β-D-glucan, and chitin [34,38]. The anomeric region of carbohydrates at 910–880 cm^{-1} is representative of the linkage of β-glycosidic bonds, such as those found in chitin and β-D-glucans, is also associated with C-H deformation [38,39]. Additionally, two IR bands at 1650–1632 cm^{-1} (amide I) and 1554–1535 cm^{-1} (am-ide II) were linked to the amide vibrations in chitin and proteins, with the amide I band partially overlapping with the water in-plane deformation band near 1640 cm^{-1} [36]. A peak at 1726 cm^{-1} was also detected, corresponding to the C=O stretching vibrations of carboxylic

groups in chitin. The bands at 1461–1455 cm^{-1} and 1374–1367 cm^{-1} were attributed to the bending vibrations of CH_2 and CH_3 groups in proteins and polysaccharides [38–40]. The band at 1372 cm^{-1} was assigned to the stretching vibration of the amide N–C bond [40,41].

Table 2. ATR-FTIR data for the 4 types of non-treatment mushroom strains.

No.	Component	Wavenumber (cm^{-1})	Ref.
1	Polysaccharides (Chitin, glucans)	1372, 1322, 1250, 1200, 1150, 1076–1071, 1040–1033, 1020, 910–880	[34–40]
2	Proteins	1650–1632, 1554–1535	[36]
3	Lipids	2930, 2868	[40]
4	Phosphates	1407–1150	[24,41]
5	Water and Hydrogen bond	3280 (broad)	[40]

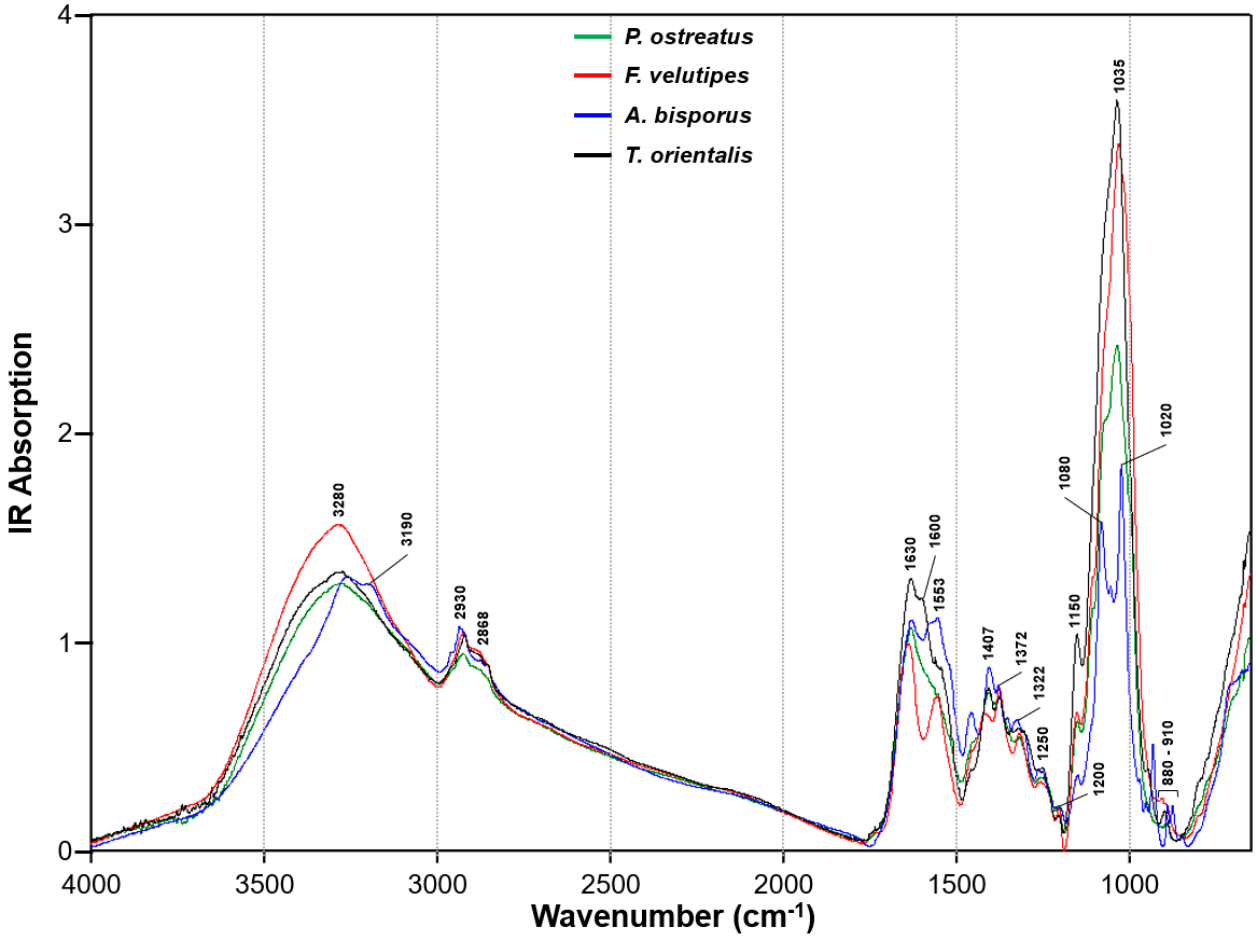


Figure 2. ATR-FTIR spectra for the 4 types of non-treatment mushroom strains: *Pleurotus ostreatus* (green); *Flammulina velutipes* (red); *Agaricus bisporus* (blue); *Trametes orientalis* (black).

The broad and intense peak observed in the 3700–3000 cm^{-1} region is typically attributed to moisture and hydroxyl groups [40]. This spectral region can exhibit variations depending on the FT-IR measurement technique employed. Common approaches include the use of KBr pellet compression and ATR. The KBr method tends to result in a stronger peak signal than ATR, primarily due to the higher moisture absorption during sample preparation and measurement. Consequently, differences in spectral patterns can be observed based on the chosen technique. Additionally, while a sharp and strong peak

corresponding to primary amines can be detected in this region, it is often obscured by signals from hydrogen bonding. Notably, *A. bisporus* has been observed to exhibit amine characteristics more prominently compared to other strains.

However, after decolorization, no significant changes in the peak bands were observed before and after physicochemical treatment for all mushrooms except *A. bisporus*. Thus, chemical composition changes could not be detected by FT-IR spectra (Figure 3) [24]. In the case of *A. bisporus*, significant differences in the spectra were observed following chemical treatment, particularly with substantial changes occurring before 1500 cm^{-1}. A sharp peak was observed at 1465 cm^{-1} after pretreatment, which is believed to result from the high reactivity of the hyphae due to the chemical treatment. NaOH, being a solid base, saponifies the lipids within the hyphae, forming salts. The aliphatic methylene (-CH_2-) groups produced in this process are likely responsible for the strong peak at 1465 cm^{-1} in the FT-IR spectrum [39]. Additionally, a peak was observed at 1319 cm^{-1} in the same strain, which is attributed to forming a new carboxyl group (C-O) stretching vibration [36]. This was likely due to the binding of sodium oxalate to the functional groups within the cell wall components during treatment.

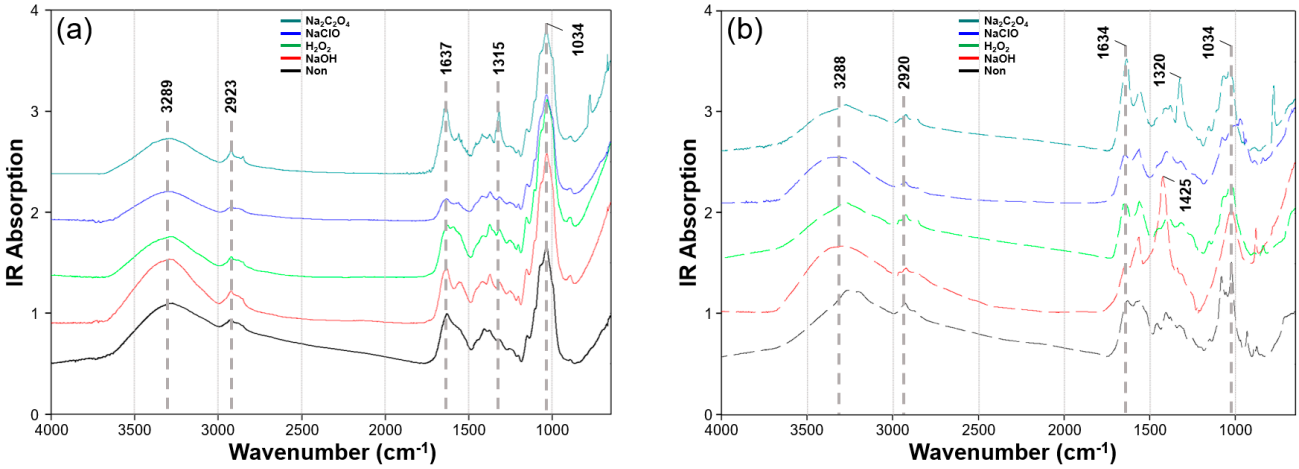


Figure 3. ATR-FTIR spectra of non-treatment and DMPs. (**a**) *Pleurotus ostreatus* (solid line); (**b**) *Agaricus bisporus* (Long dash): Non-treatment (black); pretreatment (red); H_2O_2 decolorization (green); NaClO decolorization (blue); $Na_2C_2O_4$ decolorization (dark cyan).

3.3. Crystalline Structure

XRD analysis is primarily utilized to examine crystalline structures within materials. In this study, consistent with previous research, the XRD spectrum exhibited a broad peak in the 17–23° region (Figure 4a), primarily attributed to the amorphous regions of β-glucan [42,43]. Typically, chitin displays strong and sharp peaks around 10° and 20° [44]. In the case of *T. orientalis*, sharp peaks were observed at 9.7° and 20.3° in the untreated sample, indicating the presence of crystalline chitin within the structure. These differences are presumed to arise from the variations in the mushroom form (fruiting body, mycelium). According to the studies by Ospina Alvarez et al. and Luo et al. [45,46], XRD structural analysis of *Ganoderma lucidum* revealed that the fruiting body exhibited an amorphous region with a peak at 19.56°, which is consistent with the results for the two fruiting bodies used in this study. In contrast, the analysis of the mycelium showed a sharp peak in the region corresponding to the chitin crystalline structure. These findings provide a critical basis for explaining the variations observed in this study.

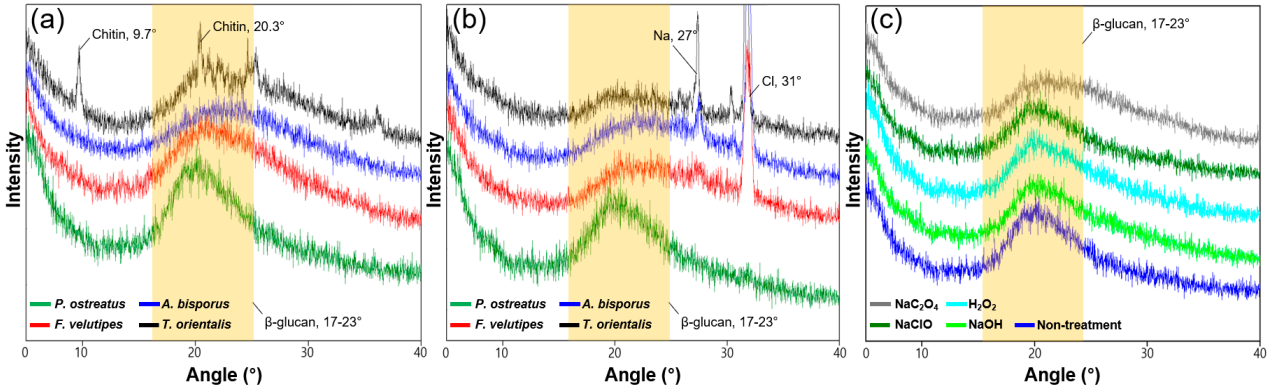


Figure 4. XRD spectra of DMPs. (**a**) non-treated mushroom pulp; (**b**) 4 types of DMPs with NaClO treatment: *Pleurotus ostreatus* (green); *Flammulina velutipes* (red); *Agaricus bisporus* (blue); *Trametes orientalis* (black); (**c**) *P. ostreatus* DMPs: Non-treatment (black); pretreatment (red); H_2O_2 decolorization (green); NaClO decolorization (blue); $Na_2C_2O_4$ decolorization (dark cyan).

Similarly to the FT-IR results, no significant differences were observed between untreated DMPs, nor were any substantial changes detected before and after chemical treatment (Figure 4c). However, in the NaClO-treated samples, *A. bisporus* and *T. orientalis* exhibited lower efficiency in salt removal during the washing process, leading to the observation of salt peaks at 27° (Na^+) and 31° (Cl^-) due to residual salt not being removed during washing (Figure 4b). Ultimately, the XRD analysis revealed a broad peak around 20°, supporting the conclusion that the mushroom structure contains significant amorphous regions. This finding aligns with the generally amorphous nature of the polysaccharides within the mushrooms, as previously discussed [43,47].

3.4. Color

Decolorization refers to altering chromophores' structures within mushroom and fungal pigments, as shown in Figure 5a, allowing an object to display color, thereby changing the molecule's energy absorption characteristics within the molecule [48]. Chromophores, typically containing polyene and aromatic compounds, possess conjugated systems that enable electron delocalization across the molecule or a significant portion of it [49]. This electron delocalization allows the molecule to absorb light at specific wavelengths, resulting in the appearance of color. The absorption spectrum can be shifted by altering the conjugated system, leading to the loss of color [50]. The color white is often preferred for nonwoven fabrics for several reasons, such as versatility, optical properties, cleanliness perception, visibility of contamination, temperature regulation, and esthetic neutrality. The choice of color ultimately depends on the nonwoven fabric's specific application and desired properties. To analyze the effects of decolorant, as illustrated in Figure 5b, treatment on different mushrooms, CIELAB color parameters (L*, a*, b*) were measured.

Figure 6 summarizes the color parameters of DMPs analyzed using a colorimeter and Table 3. shows the statistical significance analysis data. The data indicate that, following decolorant treatment, the fruiting body showed the highest efficiency with H_2O_2 treatment, while the mycelium, *T. orientalis*, demonstrated the highest efficiency with NaClO treatment. However, due to its inherently higher whiteness, the mycelium exhibited a relatively lower decolorization efficiency than the fruiting body. The exact cause of this phenomenon remains unclear. Future studies will aim to clarify the underlying reasons through component analysis of fruiting bodies and mycelial mats and experiments examining the impact of hyphal structure on decolorization. These studies will allow for a more detailed performance analysis according to strain, hyphal structure, and mushroom form.

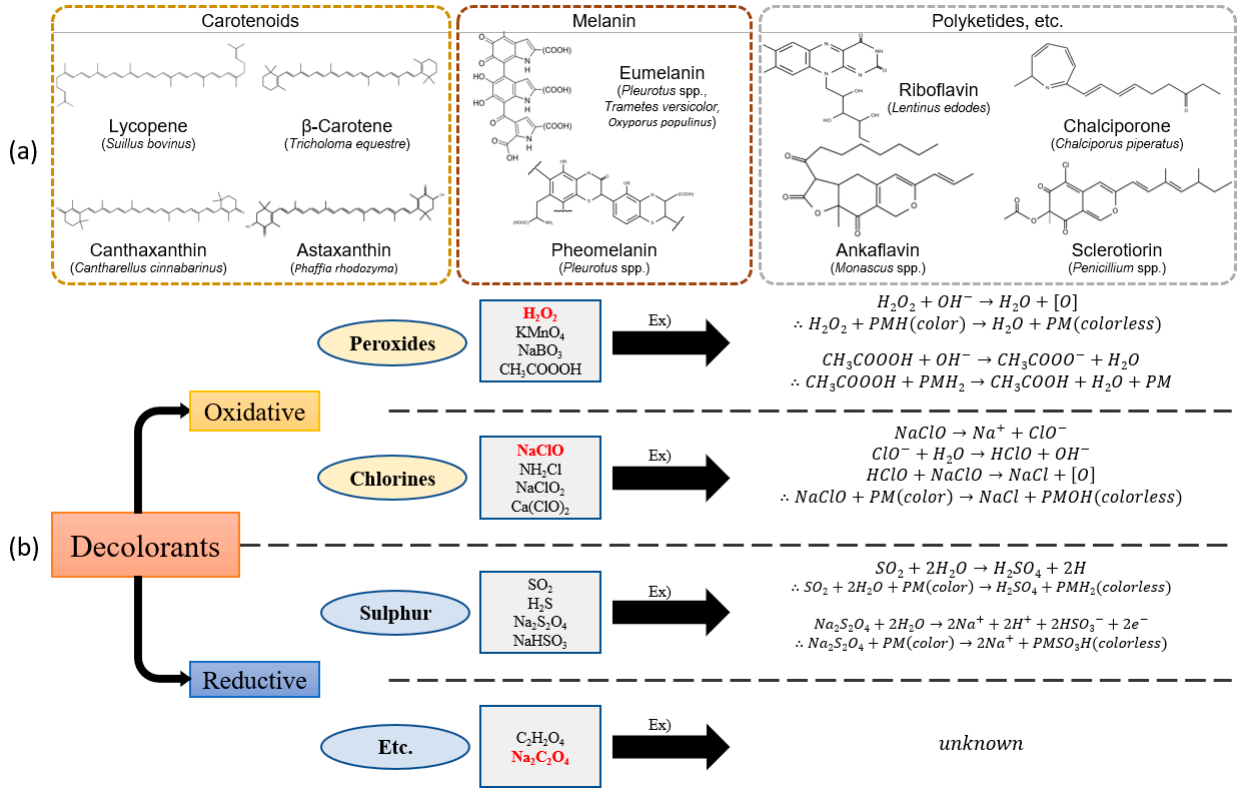


Figure 5. Illustrations of fungal pigments and decolorants. (**a**) Reported mushroom and fungal pigments; (**b**) classification of decolorants (PM; abbreviation of pigments, Red; using agents in this study).

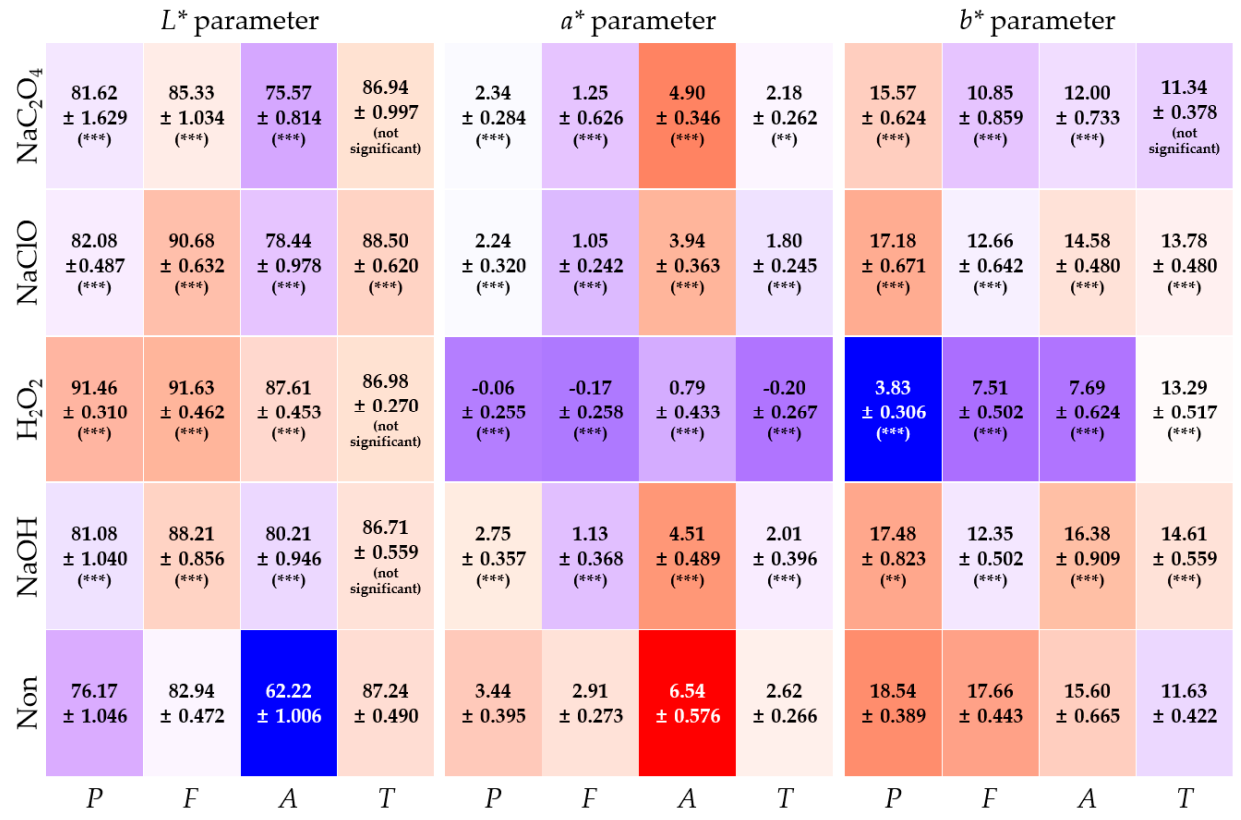


Figure 6. Mean heatmap of color parameters for different treatments and fungal strains (data: mean ± standard deviation; Non; Non treated strain, NaOH; NaOH pretreatment, H_2O_2; H_2O_2 treatment

after pretreatment, NaClO; NaClO treatment after pretreatment, $Na_2C_2O_4$; $Na_2C_2O_4$ treatment after pretreatment, P; *Pleurotus ostreatus*, F; *Flammulina velutipes*, A; *Agaricus bisporus*, T; *Trametes orientalis*). Data are presented as the average of N = 10 for each section (**: $p \leq 0.01$; ***: $p \leq 0.001$).

Table 3. Statistical significance analysis of color parameters based on *p*-values using the Tukey HSD test among DMPs.

	Pleurotus ostreatus				***Flammulina velutipes***			
	[a] Non	**NaOH**	**H_2O_2**	**NaClO**	**Non**	**NaOH**	**H_2O_2**	**NaClO**
[b] NaOH	L* < 0.001 a* < 0.001 b* < 0.01				L* < 0.001 a* < 0.001 b* < 0.001			
[c] H_2O_2	L* < 0.001 a* < 0.001 b* < 0.001	L* < 0.001 a* < 0.001 b* < 0.001			L* < 0.001 a* < 0.001 b* < 0.001	L* < 0.001 a* < 0.001 b* < 0.001		
[d] NaClO	L* < 0.001 a* < 0.001 b* < 0.001	L*: 0.198 a* < 0.001 b*: 0.790	L* < 0.001 a* < 0.001 b* < 0.001		L* < 0.001 a* < 0.001 b* < 0.001	L* < 0.001 a*: 0.990 b*: 0.773	L* < 0.05 a* < 0.001 b* < 0.001	
[e] $Na_2C_2O_4$	L* < 0.001 a* < 0.001 b* < 0.001	L*:0.758 a*: 0.054 b* < 0.001	L* < 0.001 a* < 0.001 b* < 0.001	L*: 0.848 a*: 0.959 b* < 0.001	L* < 0.001 a* < 0.001 b* < 0.001	L* < 0.001 a*: 0.955 b* < 0.001	L* < 0.001 a* < 0.001 b* < 0.001	L* < 0.001 a*: 0.766 b* < 0.001
	Agaricus bisporus				*Trametes orientalis*			
	Non	NaOH	H_2O_2	NaClO	Non	NaOH	H_2O_2	NaClO
NaOH	L* < 0.001 a* < 0.001 b* < 0.001				L*: 0.336 a* < 0.001 b* < 0.001			
H_2O_2	L* < 0.001 a* < 0.001 b* < 0.001	L* < 0.001 a* < 0.001 b* < 0.001			L*: 0.933 a* < 0.001 b* < 0.001	L*: 0.802 a* < 0.001 b* < 0.001		
NaClO	L* < 0.001 a* < 0.001 b* < 0.001	L* < 0.001 a*: 0.051 b*: 0.114	L* < 0.001 a* < 0.001 b* < 0.001		L* < 0.001 a* < 0.001 b* < 0.001	L* < 0.001 a*: 0.519 b* < 0.01	L* < 0.001 a* < 0.001 b*: 0.163	
$Na_2C_2O_4$	L* < 0.001 a* < 0.001 b* < 0.001	L* < 0.001 a*: 0.311 b*: 0.447	L* < 0.001 a* < 0.001 b* < 0.001	L* < 0.001 a* < 0.001 b* < 0.001	L*: 0.820 a* < 0.05 b*: 0.654	L*: 0.923 a*: 0.706 b* < 0.001	L*: 0.998 a* < 0.001 b* < 0.001	L* < 0.001 a* < 0.05 b* < 0.001

[a] Non treated strains; [b] NaOH pretreatment; [c] H_2O_2 treatment after pretreatment; [d] NaClO treatment after pretreatment; [e] $Na_2C_2O_4$ treatment after pretreatment.

In the chemical treatment of fungal pigments to produce DMPs, H_2O_2 was generally the most effective. Using dye decoloring peroxidase (DyPs) can further improve the decolorization efficiency [51]. DyPs have shown high oxidative activity in textile dye wastewater treatment and lignin degradation, and some have also shown effectiveness in the degradation of pigments such as melanin. Therefore, DyPs are promising enzymes for color reduction in fungal pigments, and their optimization can potentially contribute to developing environmentally friendly processes and biodegradable materials. In addition, glutathione peroxidase (GPX) and thiol peroxidase (TPX) are enzymes that can effectively reduce melanin pigment by combining with H_2O_2, and have high decolorization efficiency [52].

DyPs, GPX and TPX each have unique enzymatic properties and have the potential to be complementary in the treatment of fungal pigments and synthetic dyes. DyPs are specialized in the degradation of polymeric compounds such as lignin and synthetic dyes, as well as dye wastewater or lignin-based materials. GPX and TPX, on the other hand, are effective in the decolorization of natural pigments such as melanin, and achieve high decolorization efficiency by combining with H_2O_2. A hybrid process combining these

enzymes can be developed to simultaneously remove fungal and synthetic pigments. This is a new approach to achieving high efficiency and sustainability in dye and pigment wastewater treatment. While enzymes have the advantage of lowering the energy barrier of chemical reactions and accelerating reactions, they have the disadvantage of being expensive, which increases the cost of the process, and further research is needed to optimize the reaction conditions [53].

We believe a more advanced process can be considered using the aforementioned experimental methods and the above points. In the existing process, a NaOH solution is simply added in the pretreatment, and the primary bleaching is performed using sodium borohydride ($NaBH_4$), which is bleached under basic conditions and has high stability [54]. If H_2O_2 is used for secondary bleaching, stirred under UV irradiation conditions, or reacted by adding the peroxidase mentioned above, it can be judged that it will have a higher bleaching efficiency at the same processing time. This convergent utilization is expected to contribute to developing environmentally friendly technologies in various industries.

However, although the fungal pigments were chemically modified in this study, it was found that these pigments basically serve to protect the fruiting bodies from the external environment and contain various pharmacological components such as antioxidant and anti-inflammatory effects [55–57]. However, future studies could consider how to efficiently extract and utilize these components while reducing the color of the mushrooms and conducting chemical treatments under milder conditions.

3.5. Nonwoven Fabrication

Using the fabrication equipment, the *F. velutipes* nonwoven DMP was successfully created as film-like, as shown in Figure 7a. Macroscopic DMP with defibration treatment was capable of forming sheets. This result contrasts with the outcomes from other methods using micro-scale mushroom pulp, where the process failed to properly bond the mycelium, resulting in dust-like products that could not be formed into films or other structures [24]. These findings indicate the necessity of scaling up the pulp diameter. Additionally, the film produced by this process showed similarities to the findings of Vadivel et al., likely due to the use of similar treatment processes and materials [58]. In this experiment, the sheet former was used to compress the dispersed mushroom pulp into a nonwoven sheet, followed by applying a high-temperature (120 °C) roller, which resulted in the formation of a film through the thermal deformation of the hyphae. Figure 7b shows the CLSM image of the dried nonwoven fabric formed from macroscopic DMP. The hyphae were tightly interconnected, though slight boundaries between hyphae could be observed. This indicates that the DMP nonwoven fabric sheet retains the hyphal structure [59,60].

In the wet-laid nonwoven manufacturing process, key factors in process control include the fiber dimensions and the degree of dispersion, which significantly influence the mechanical properties of the textile. Fibers used in nonwovens typically have a thickness between 3 and 7 mm, with lengths not exceeding 35 mm [61]. Surfactants play a critical role in enhancing dispersion, ensuring that fibers are uniformly distributed within the solution [62]. This uniformity is vital for producing high-quality nonwoven fabrics with consistent properties across the material. Additionally, achieving homogeneity in fiber distribution during the manufacturing process directly impacts the nonwoven fabric's tensile strength, elongation, and overall durability [59]. Therefore, proper surfactant selection and fiber size control are essential for maintaining product quality and optimizing the final material's functional characteristics. Further studies should focus on refining the surfactant compositions and examining their long-term effects on the mechanical stability and biodegradability of biotextiles.

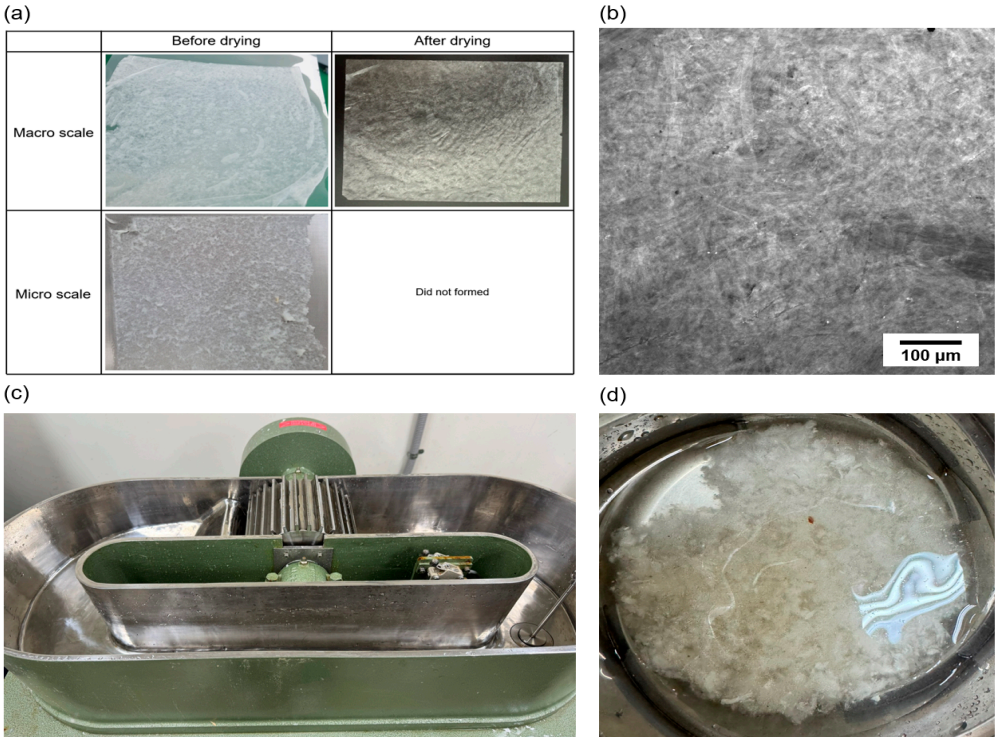


Figure 7. Results of nonwoven cotton and DMP sheet forming process: (**a**) pure DMP nonwoven fabrication; (**b**) a CLSM image of drying nonwoven sheet forming by macro scale DMP; (**c**) picture of beater machine; (**d**) aggregated cotton fiber during stirring process.

The nonwoven fabrication process follows the stages of stirring, beating (Figure 7c), sheet forming, and calendaring [28]. In the stirring stage, a propeller-type impeller is used to mix the pulp solution in a cylindrical tank, which serves as the initial dispersion step. However, for fibers with natural curls, such as cotton fibers, twisting between fibers often causes partial clumping (Figure 7d). Due to this issue, the stirring process was excluded from this study. The beating stage involves physical agitation through a watermill-like gear in a circulation tank, as shown in Figure 7c, further dispersing the fibers. During this process, pulps were observed to be pulverized by the impact. Specifically, DMP was found to be fragmented during the beating stage, so it was added after cotton fiber dispersion to prevent premature breakdown. The resulting solution was then processed using a sheet former to create a predefined form, and the final nonwoven material was dried through the drying process.

The goal of this study was to produce DMP using various mushrooms and to fabricate cotton-DMP nonwoven composites using them. Among the pulp produced by each strain, *P. ostreatus* and *F. velutipes* were capable of nonwoven fabrication. Based on the characteristics and associations of the strains so far, these two strains are characterized by growing long, aligned grains during fruiting body formation. On the other hand, *A. bisporus*, which was difficult to fabricate, has a short fruiting body with a coarse structure, and *T. orientalis* uses mycelial mats to form an essentially three-dimensional matrix structure. This difference in the raw material formation process is likely a major factor in the success of nonwoven fabrication in *P. ostreatus* and *F. velutipes*.

When scaling up DMP to mass production, we believe there are two main areas to consider. The first is the non-uniformity of process parameters that occurs when transitioning from laboratory to industrial scale [63,64]. In laboratory conditions, we utilize a relatively small scale (~5 L), so there are no major restrictions on material exchange, but we believe that scaling up to industrial scale may result in partially different material concentrations,

which may affect pulp quality. The second is the supply of raw materials. However, this problem can be solved by utilizing mycelium instead of mushroom fruiting bodies. Mycelium can be mass cultured in a controlled environment, ensuring a stable and sustainable supply of raw materials for industrial applications. The utilization of mycelium has the potential to replace or complement existing mushroom fruiting body-based processes, and it is essential to optimize it through future research.

Based on the LCA analysis of various researchers using mushroom mycelium materials, they recognized the potential of mycelium as an excellent material for circular economy and sustainability [18–20]. In particular, they agree that utilizing biomass by-products and recycled materials can further increase the environmental efficiency of alternative materials [18,65]. In the cultivation of mushroom fruiting bodies, the thinning process is an integral part of the process to produce a high-quality product, which results in small, non-commodity fruiting body by-products [66]. Utilizing these by-products to produce DMP reduces the environmental impact and serves as a virtuous cycle of resources. Furthermore, the LCA analysis of cotton fiber materials by Chen et al. (2021) found that 4.43 kg CO_2 eq. is generated per kilogram of cotton fiber produced [67], with high eutrophication and ecotoxicity due to fertilizer and pesticide use. According to Williams et al. (2022) [68], large-scale cultured mycelium-based leather manufactured to replace cowhide is expected to reduce the total carbon footprint of production by 2.76 kg CO_2 eq. As such, mushroom materials can be proven eco-friendly and reduce carbon emissions, and further research will be conducted to evaluate the environmental impact of pulp manufacturing processes. Limitations anticipated at this time include the potential for fluctuations in fruit yields due to environmental factors and disease. Fruiting bodies are sensitive to environmental changes from pathogens, which can also cause reduced yields. This variability can make it difficult to ensure a stable supply of raw materials.

Further research on the optimization of mycelium-based processes is essential to address these issues and maximize DMP's industrial potential. Such research will not only contribute to increasing DMP's commercial success but will also play an important role in the development of eco-friendly and sustainable materials for the textile industry.

3.6. Nonwoven Textile Produced from a Composite of Cotton and DMP

The nonwoven composite prepared from cotton and DMP derived from *F. velutipes* are shown in Figure 8. In the cotton-only sample (Figure 8a), gaps were observed between the fibers, likely due to the beating process. The cotton fibers experienced physical impacts during this process, leading to splitting at the fiber ends or twisting in the middle sections. The CLSM results of the composite mixed with DMP and cotton fiber showed a similar pattern to the findings reported by Rong and Bhat [69], who observed the fabrication outcomes of cotton fiber and polymer-based fiber composites. In contrast, these gaps were filled in the composite sample (Figure 8b), and the material filling these gaps is presumed to be hyphae. This suggests that combining DMP with cotton can enhance the bonding strength between fibers and control the pore size of the fabric.

The nonwoven composites produced by this process can be measured by universal testing machines and tensile testing standards for textiles, such as KS K 0520, ASTM D5034, ISO 13934-1 [70,71]. The physical properties of the tested cotton-DMP (H_2O_2 treatment sample) nonwoven composite was measured under the above standard, KS K 0520, and the data are shown in Table 4. Numerically, it was observed that the values decreased with the addition of DMP. Still, when analyzed using statistical software, it was confirmed that all cases had no significant difference. This is likely due to the lower physical properties of DMP fibers compared to cotton fibers. Cotton fibers resist when the beating process is applied during nonwoven fabrication, while DMP fibers are all shredded. A study by Flores

et al. (2024) showed that the chemical treatment of jute fiber composites did not promote an increase in overall properties [72], and that chemical treatments are not universally the same in studies in the literature because natural fibers vary in composition depending on yield or species. As mentioned above, controlling the fiber length may increase the physical properties, which we will investigate in future studies.

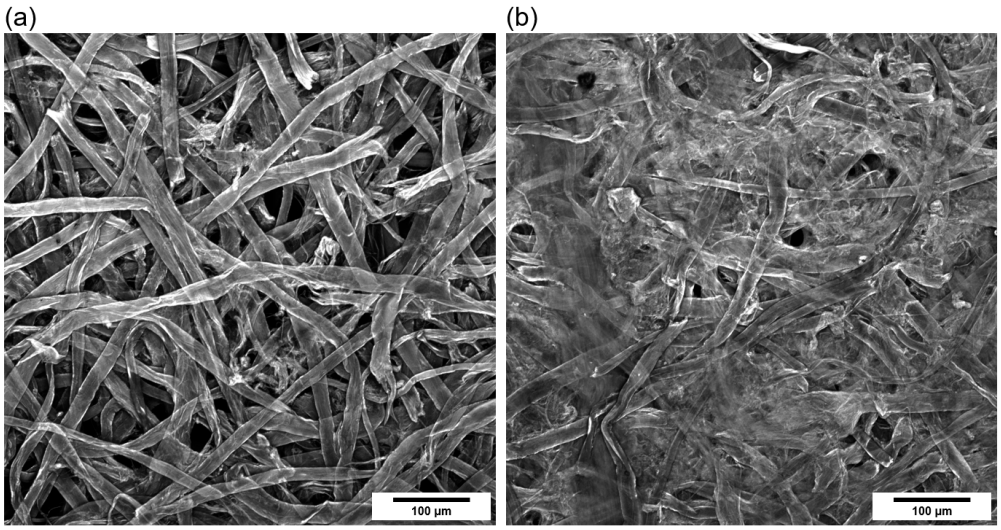


Figure 8. CLSM observation of nonwoven and composite. (**a**) cotton only; (**b**) Cotton-*Flammulina velutipes* DMP nonwoven composite.

Table 4. Cotton-DMP nonwoven composite mechanical property (data: mean ± standard deviation). Data are presented as the average of N = 3 for each specimen (ns: not statistically significant).

Specimen	Mix Ratio ([a] CF:[b] M)	Area Density (g/m^2)	Tensile Strength (MPa)	*p*-Value
CF	10:0	136.59 ± 13.761	1.097 ± 0.069 [ns]	-
CF + [c] PoD	8:2	134.56 ± 16.207	1.086 ± 0.078 [ns]	0.9763
CF + [d] FvD		130.40 ± 9.251	1.037 ± 0.057 [ns]	0.5589

[a] Cotton fiber; [b] Decolorized mushroom pulp (DMP); [c] *Pleurotus ostreatus* DMP; [d] *Flammulina velutipes* DMP.

In the future, we plan to prepare specimens with the size specified in the standard and measure data according to the test conditions to analyze various properties such as tensile strength of the textile and summarize its antibacterial ability.

4. Conclusions

Research on the production and application of pulp from mushroom fruiting bodies and mycelium is still in its infancy. In this study, four mushroom strains with different mycelium characteristics were used to produce pulp, and three different decolorants were applied to analyze the effective treatment for whitening mushrooms. The DMPs show promise as an environmentally friendly alternative to cotton fiber, and the physicochemical treatments showed little difference in composition. The DMPs were successfully combined with cotton fibers to produce nonwoven fabrics, potentially solving the environmental problems associated with cotton fiber cultivation. Future research will include investigating the performance of pulp production from mycelium and mycelium mats cultured under laboratory conditions. In addition, the same process will be applied to *Ganoderma lucidum* strains, which are widely used for experimental purposes to evaluate their properties under identical treatments. The results of these studies will help refine the treatment process to

produce fabrics with improved physicochemical properties. These improved fabrics will be further evaluated for antimicrobial activity against Gram-positive and Gram-negative bacterial strains. These efforts demonstrate that mushroom-based pulp is a sustainable and multifunctional material that offers new possibilities for textile manufacturing while addressing environmental concerns associated with traditional fiber cultivation.

Author Contributions: Conceptualization, H.-J.S. and H.-S.I.; methodology, H.-J.S. and J.-S.J.; software, H.-S.I.; validation, H.-S.I.; formal analysis, H.-S.I. and S.T.; investigation, H.-S.I., J.-S.J. and H.-J.S.; resources, J.-S.J. and S.T.; writing—original draft preparation, H.-S.I.; writing—review and editing, S.T., J.-S.J. and H.-J.S.; visualization, H.-S.I. and S.T.; project administration, H.-J.S.; funding acquisition, H.-J.S. All authors have read and agreed to the published version of the manuscript.

Funding: This study was supported by research fund from Chosun University, 2024.

Data Availability Statement: The original contributions presented in the study are included in the article, further inquiries can be directed to the corresponding author.

Acknowledgments: The authors would like to thank Korea Institute of Industrial Technology for providing the equipment necessary for the fabrication of pure DMP nonwovens.

Conflicts of Interest: The authors declare no conflicts of interest.

References

1. World Meteorological Organization (WMO). Available online: https://wmo.int/publication-series/state-of-global-climate-2023 (accessed on 1 September 2024).
2. Chang, A.K.; Hoekstra, A.Y.; Savenije, H.H.G.; Gautam, R. The water footprint of cotton consumption: An assessment of the impact of worldwide consumption of cotton products on the water resources in the cotton producing countries. *Ecol. Econ.* **2006**, *60*, 186–203.
3. Jans, Y.; Bloh, W.V.; Schaphoff, S.; Müller, C. Global cotton production under climate change implications for yield and water consumption. *Hydrol. Earth Syst. Sci.* **2021**, *25*, 2027–2044. [CrossRef]
4. Altenbuchner, C.; Vogel, S.; Larcher, M. Social, economic and environmental impacts of organic cotton production on the livelihood of smallholder farmers in Odisha, India. *Renew. Agric. Food Syst.* **2018**, *33*, 373–385. [CrossRef]
5. Li, N.; Li, Y.; Biswas, A.; Wang, J.; Dong, H.; Chen, J.; Liu, C.; Fan, X. Impact of climate change and crop management on cotton phenology based on statistical analysis in the main-cotton-planting areas of China. *J. Clean. Prod.* **2021**, *298*, 126750. [CrossRef]
6. Gao, Y.; Serrenho, A.C. Greenhouse gas emissions from nitrogen fertilizers could be reduced by up to one-fifth of current levels by 2050 with combined interventions. *Nat. Food* **2023**, *4*, 170–178. [CrossRef]
7. Akromah, S.; Chandarana, N.; Eichhorn, S.J. Mycelium composites for sustainable development in developing countries: The case of Africa. *Adv. Sustain. Syst.* **2024**, *8*, 2300305. [CrossRef]
8. Raman, J.; Kim, D.S.; Kim, H.S.; Oh, D.S.; Shin, H.J. Mycofabrication of mycelium-based leather from brown-rot fungi. *J. Fungi* **2022**, *8*, 317. [CrossRef]
9. Mazumder, M.A.R.; Sukchot, S.; Phonphimai, P.; Ketnawa, S.; Chaijan, M.; Grossmann, L.; Rawdkuen, S. Mushroom-legume-based minced meat: Physico-chemical and sensory properties. *Foods* **2023**, *12*, 2094. [CrossRef]
10. Zhang, X.; Hu, J.; Fan, X.; Yu, X. Naturally grown mycelium-composite as sustainable building insulation materials. *J. Clean. Prod.* **2022**, *342*, 130784. [CrossRef]
11. Suwannarach, N.; Kumla, J.; Zhao, Y.; Kakumyan, P. Impact of cultivation substrate and microbial community on improving mushroom productivity: A review. *Biology* **2022**, *11*, 569. [CrossRef]
12. Rathore, H.; Prasad, S.; Kapri, M.; Tiwari, A.; Sharma, S. Medicinal importance of mushroom mycelium: Mechanisms and applications. *J. Funct. Foods* **2019**, *56*, 182–193. [CrossRef]
13. Porter, D.L.; Naleway, S.E. Hyphal systems and their effect on the mechanical properties of fungal systems. *Acta Biomater.* **2022**, *145*, 272–282. [CrossRef]
14. Bhambri, A.; Srivastava, M.; Mahale, V.G.; Mahale, S.; Karn, S.K. Mushrooms as potential sources of active metabolites and medicines. *Front. Microbiol.* **2022**, *13*, 837266. [CrossRef]
15. Zhang, Y.; Wu, X.; Huang, C.; Zhang, Z.; Gao, W. Isolation and identification of pigments from oyster mushrooms with black, yellow and pink caps. *Food Chem.* **2022**, *372*, 131171. [CrossRef] [PubMed]
16. Lin, L.; Xu, J. Fungal pigments and their roles associated with human health. *J. Fungi* **2020**, *6*, 280. [CrossRef] [PubMed]
17. Esatbeyoglu, T.; Rimbach, G. Canthaxanthin: From molecule to function. *Mol. Nutr. Food Res.* **2017**, *61*, 1600469. [CrossRef]

18. Alaux, N.; Vašatko, H.; Malerhofer, D.; Saade, M.R.M.; Stavrlc, M.; Passer, A. Environmental potential of fungal insulation: A prospective life cycle assessment of mycelium-based composites. *Int. J. Life Cycle Assess.* **2024**, *29*, 255–272. [CrossRef]
19. Enarevba, D.R.; Haapala, K.R. A comparative life cycle assessment of expanded polystyrene and mycelium packaging box inserts. *Procedia CIRP* **2023**, *116*, 654–659. [CrossRef]
20. Akromah, S.; Chandarana, N.; Rowlandson, J.L.; Eichhorn, S.J. Potential environmental impact of mycelium composites on African communities. *Sci. Rep.* **2024**, *14*, 11867. [CrossRef]
21. National Institute of Horticultural and Herbal Science. Available online: https://www.nihhs.go.kr/farmer/statistics/statistics.do?t_cd=0206 (accessed on 10 January 2025).
22. Jeong, Y.H.; Kim, D.S.; Kim, H.S.; Oh, D.S.; Shin, H.J. Effect of culture and method and medium components on *Trametes orientalis* mycelium mat formation (Yasuda) Imazeki. *J. Mushrooms* **2022**, *20*, 69–77.
23. Da Silva, C.J.G.; de Medeiros, A.D.L.M.; de Amorim, J.D.P.; do Nascimento, H.A.; Converti, A.; Costa, A.F.S.; Sarubbo, L.A. Bacterial cellulose biotextiles for the future of sustainable fashion: A review. *Environ. Chem. Lett.* **2021**, *19*, 2967–2980. [CrossRef]
24. Somogyi Škoc, M.; Stevelić, N.; Rezić, I. Development and characterization of sustainable coatings on cellulose fabric and nonwoven for medical applications. *Sustainability* **2024**, *16*, 857. [CrossRef]
25. Rizwan, M.; Gilani, S.R.; Durrani, A.I.; Naseem, S. Cellulose extraction of *Alstonia scholaris*: A comprarative study on efficiency of different bleaching reagents for its isolation and characterization. *Int. J. Biol. Macromol.* **2021**, *191*, 964–972. [CrossRef] [PubMed]
26. Nakauchi, H.; Amano, Y.; Tagawa, S. Preparation of mycelium pulp from mushroom fruiting bodies. *ACS Sustain. Chem. Eng.* **2023**, *11*, 15789–15794. [CrossRef]
27. Jeong, Y.H.; Kim, D.S.; Shin, H.J. *Trametes orientalis* mycelium mat, can be used as an alternative to elastomers? *Biotechnol. Bioprocess Eng.* **2023**, *28*, 602–611. [CrossRef]
28. Yoon, M.J.; Doh, S.J.; Im, J.N. Preparation and characterization of carboxymethyl cellulose nonwovens by a wet-laid process. *Fibers Polym.* **2011**, *12*, 247–251. [CrossRef]
29. Fischer, M.W.F.; Money, N.P. Why mushrooms form gills: Efficiency of the lamellate morphology. *Fungal Biol.* **2010**, *114*, 57–63. [CrossRef]
30. Wang, C.S.; Virgilio, N.; Carreau, P.J.; Heuzey, M.C. Understanding the effect of conformational rigidity on rheological behavior and formation of polysaccharide-based hybrid hydrogels. *Biomacromolecules* **2021**, *22*, 4016–4026. [CrossRef]
31. Nawaz, R.; Naqvi, S.T.R.; Fatima, B.; Zulfiqar, N.; Farooq, M.U.; Haq, M.N.; Hussain, D.; Javeed, A.; Rasul, A.; Jafri, L.; et al. Cost-effective fabrication, antibacterial application and cell viability studies of modified nonwoven cotton fabric. *Sci. Rep.* **2022**, *12*, 2493. [CrossRef]
32. Kurita, K. Controlled functionalization of polysaccharide chitin. *Prog. Polym. Sci.* **2001**, *26*, 1921–1971. [CrossRef]
33. Gómez-Salazar, J.A.; Galván-Navarro, A.; Lorenzo, J.M.; Sosa-Morales, M.E. Ultrasound effect on salt reduction in meat products: A review. *Curr. Opin. Food Sci.* **2021**, *38*, 71–78. [CrossRef]
34. Baeva, E.; Bleha, R.; Sedliaková, M.; Sushytsktyi, L.; Švec, I.; Čopíková, J.; Jablonsky, I.; Klouček, P.; Synytsya, A. Evaluation of the cultivated mushroom *Pleurotus ostreatus* basidiocarps using vibration spectroscopy and chemometrics. *Appl. Sci.* **2020**, *10*, 8156. [CrossRef]
35. Bekiaris, G.; Tagkouli, D.; Koutrotsios, G.; Kalogeropoulos, N.; Zervakis, G.I. *Pleurotus* mushrooms content in glucans and ergosterol assessed by ATR-FTIR spectroscopy and multivariate analysis. *Foods* **2020**, *9*, 535. [CrossRef] [PubMed]
36. Sills, D.L.; Gossett, J.M. Using FTIR to predict saccharification from enzymatic hydrolysis of alkali-pretreated biomasses. *Biotechnol. Bioeng.* **2012**, *109*, 353–362. [CrossRef] [PubMed]
37. Bekiaris, G.; Koutrotsios, G.; Tarantilis, P.A.; Pappas, C.S.; Zervakis, G.I. FTIR assessment of compositional changes in lignocellulosic wastes during cultivation of *Cyclocybe cylindracea* mushrooms and use of chemometric models to predict production performance. *J. Mater. Cycles Waste Manag.* **2020**, *22*, 1027–1035. [CrossRef]
38. Bikmurzin, R.; Bandezevičiūtė, R.; Maršalka, A.; Maneikis, A.; Kalėdienė, L. FT-IR method limitations for β-glucan analysis. *Molecules* **2022**, *27*, 4616. [CrossRef]
39. Pandey, K.K.; Pitman, A.J. FTIR studies of the changes in wood chemistry following decay by brown-rot and white-rot fungi. *Int. Biodeterior. Biodegrad.* **2003**, *52*, 151–160. [CrossRef]
40. Coates, J. Interpretation of infrared spectra: A practical approach. In *Encyclopedia of Analytical Chemistry*; Meyers, R.A., Ed.; John Wiley & Sons Ltd.: Chichester, UK, 2000; pp. 10815–10837.
41. Pylkkänen, R.; Werner, D.; Bishoyl, A.; Well, D.; Scoppola, E.; Wagermaler, W.; Safeer, A.; Bahrl, S.; Baldus, M.; Paananen, A.; et al. The complex structure of *Fomes fomentarius* represents an architectural design for high-performance ultralightweight materials. *Sci. Adv.* **2023**, *9*, eade5417. [CrossRef]
42. Shams, R.; Singh, J.; Dash, K.K.; Dar, A.H. Comparative study of freeze drying and cabinet drying of button mushroom. *Appl. Food Res.* **2022**, *2*, 100084. [CrossRef]
43. Wang, W.; Li, C.; Zhang, X.; Zhang, H. Characteristics and rheological properties of polysaccharide nanoparticles from edible mushrooms (*Flammulina velutipes*). *J. Food Sci.* **2017**, *82*, 687–693. [CrossRef]

44. Cárdenas, G.; Cabrera, G.; Taboada, E.; Miranda, S.P. Chitin characterization by SEM, FTIR, XRD and ^{13}C cross polarization/mass angle spinning NMR. *J. Appl. Polym. Sci.* **2004**, *93*, 1876–1885. [CrossRef]
45. Ospina Álvares, S.P.; Ramírez Cadavid, D.A.; Escobar Sierra, D.M.; Ossa Orozco, C.P.; Rojas Vahos, D.F.; Zapata Ocampo, P.; Atehortúa, L. Comparison of extraction methods of chitin from *Ganoderma lucidum* mushroom obtained in submerges culture. *BioMed Res. Int.* **2014**, *2014*, 169071.
46. Xu, L.; Sun, J.; Qaria, M.A.; Gao, L.; Zhu, D. Dye decoloring peroxidase structure, catalytic properties and applications: Current advancement and futurity. *Catalysts* **2021**, *11*, 955. [CrossRef]
47. Jeon, G.C.; Kim, C.H.; Cho, U.M.; Hwang, E.T.; Hwang, H.S.; Min, J.H. Melanin-decoloring activity of antioxidant enzymes, glutathione peroxidase, thiol peroxidase, and catalase. *Mol. Biotechnol.* **2021**, *63*, 150–155. [CrossRef] [PubMed]
48. Toma, M.A.; Rahman, M.H.; Rahman, M.S.; Arif, M.; Nazir, K.H.M.N.; Dufossé, L. Fungal pigments: Carotenoids, riboflavin, and polyketides with diverse applications. *J. Fungi* **2023**, *9*, 454. [CrossRef]
49. Molelekoa, T.; da Silva, L.S.; Regnier, T.; Augustyn, W. Application and stability of fungal pigments using jellysweets as a food model system. *Food Sci Technol.* **2023**, *58*, 6761–6774.
50. Bayram, S.; Aygün, B.; Karadayi, M.; Alaylar, B.; Güllüce, M.; Karabulut, A. Determination of toxicity and radioprotective properties of bacterial and fungal eumelanin pigments. *Int. J. Radiat. Biol.* **2023**, *99*, 1785–1793. [CrossRef]
51. Luo, H.J.; Zhan, Y.K.; Wang, S.Z.; Lin, S.Q.; Wang, L.F.; Lin, Z.X.; Lu, G.D.; Lin, D.M. Structural characterization and anti-oxidative activity for a glycopeptide from *Ganoderma lucidum* fruiting body. *Int. J. Biol. Macromol.* **2024**, *261*, 129793. [CrossRef]
52. Ifuku, S.; Nomura, R.; Morimoto, M.; Saimoto, H. Preparation of chitin nanofibers from mushrooms. *Materials* **2011**, *4*, 1417–1425. [CrossRef]
53. Chapman, J.; Ismail, A.E.; Dinu, C.Z. Industrial applications of enzymes: Recent advances, techniques, and outlooks. *Catalysts* **2018**, *8*, 238. [CrossRef]
54. Lehto, J.; Heiningen, A.V.; Patil, R.; Louhelainen, J.; Alén, R. Effect of sodium borohydride and hydrogen peroxide pretreatments on soda pulping of sugar maple (*Acer saccharum*). *JWCT* **2021**, *41*, 128–136. [CrossRef]
55. Farr, J.P.; Smith, W.L.; Steichen, D.S. Bleaching agents. In *Kirk-Othmer Encyclopedia of Chemical Technology*; John Wiley & Sons: Hoboken, NJ, USA, 2003; pp. 43–81.
56. Yi, H.; Qin, X.; Zhai, L.; Duan, H.; Chen, H.; Zuo, Y.; Lian, X.; Tian, K.; Zhang, J.; Liu, Z.; et al. Positional isomeric thiophene-based π-conjugated chromophores: Synthesis, structure, and optical properties. *Precis. Chem.* **2023**, *1*, 548–554. [CrossRef]
57. Li, R.; Yang, J.; Zhang, G.; Zhu, P. Decolorization of dark-colored waste cotton fabric using redox decoloring agents. *RSC Adv.* **2022**, *12*, 17689–17700. [CrossRef] [PubMed]
58. Vadivel, D.; Cartabia, M.; Scalet, G.; Buratti, S.; Landro, L.D.; Benedetti, A.; Auricchio, F.; Babbini, S.; Savino, E.; Dondi, D. Innovative chitin-glucan based material obtained from mycelium of wood decay fungal strains. *Heliyon* **2024**, *10*, e28709. [CrossRef] [PubMed]
59. Venu, L.B.S.; Shim, E.; Anantharamaiah, N.; Pourdeyhimi, B. Three-dimensional structural characterization of nonwoven fabrics. *Microsc. Microanal.* **2012**, *18*, 1368–1379. [CrossRef] [PubMed]
60. Karunarathne, A.; Nabiyeva, G.; Rasmussen, C.J.; Alkhoury, K.; Assem, N.; Bauer, J.; Chester, S.A.; Khalizov, A.F.; Gor, G.Y. Effects of humidity on mycelium-based leather. *ACS Appl. Bio Mater.* **2024**, *7*, 6441–6450. [CrossRef] [PubMed]
61. Hubbe, M.A.; Koukoulas, A.A. Wet-laid nonwovens manufacture-Chemical approaches using synthetic and cellulosic fibers. *BioResources* **2016**, *11*, 5500–5552. [CrossRef]
62. Kang, Y.J.; Song, S.H. Effects of surfactants on dispersion behavior of Vectran® in water (II)-Study on the manufacture and properties of wet-laid fabrics-. *Text. Color. Finish.* **2015**, *27*, 327–333. [CrossRef]
63. Seidel, S.; Mozaffari, F.; Maschke, R.W.; Kraume, M.; Eibl-Schindler, R.; Eibl, D. Automated shape and process parameter optimization for scaling up geometrically non-similar bioreactors. *Processes* **2023**, *11*, 2703. [CrossRef]
64. Xia, J.Y.; Wang, G.; Lin, J.H.; Wang, Y.H.; Chu, J.; Zhuang, Y.P.; Zhang, S.L. Advances and Practices of Bioprocess Scale-up. In *Bioreactor Engineering Research and Industrial Applications II*; Bao, J., Ye, Q., Zhong, J.J., Eds.; Advances in Biochemical Engineering-Biotechnology; Springer: Berlin/Heidelberg, Germany, 2016; Volume 152, pp. 137–151.
65. Hildebrandt, J.; Thrän, D.; Bezama, A. The circularity of potential bio-textile production routes: Comparing life cycle impacts of bio-based materials used within the manufacturing of selected leather substitutes. *J. Clean. Prod.* **2021**, *287*, 125470. [CrossRef]
66. Jung, D.H.; Son, J.E. Carbon dioxide emission modeling of king oyster mushroom before and after thinning processes according to temperature and growth stage. *J. Bio-Environ. Control* **2021**, *30*, 140–148. [CrossRef]
67. Chen, F.; Ji, X.; Chu, J.; Xu, P.; Wang, L. A Review: Life Cycle Assessment of Cotton Textiles. *Ind. Textila* **2021**, *72*, 19–29. [CrossRef]
68. Williams, E.; Cenian, K.; Golsteijn, L.; Morris, B.; Scullin, M.L. Life Cycle Assessment of MycoWorks' Reishi™: The First Low-Carbon and Biodegradable Alternative Leather. *Environ. Sci. Eur.* **2022**, *34*, 120. [CrossRef]
69. Rong, H.; Bhat, G.S. Binder fiber distribution and tensile properties of thermally point bonded cotton-based nonwovens. *J. Appl. Polym. Sci.* **2004**, *91*, 3148–3155. [CrossRef]

70. Maino, A.; Janszen, G.; Di Landro, L. Glass/Epoxy and Hemp/Bio Based Epoxy Composites: Manufacturing and Structural Performances. *Polym. Compos.* **2019**, *40*, E723–E731. [CrossRef]
71. Woo, Y.E.; Oh, K.W. Fabrication of polyester fabrics with tungsten bronze nanorods and a silane coupling agent for improved thermal storage and washing durability. *Fash. Text.* **2023**, *10*, 1. [CrossRef]
72. Flores, A.L.L.; Kairytė, A.; Šeputytė-Jucikė, J.; Makowska, S.; Lavoratti, A.; de Avila Delucis, R.; Amico, S.C. Effect of chemical treatments on the mechanical properties of jute/polyester composites. *Materials* **2024**, *17*, 2320. [CrossRef]

Disclaimer/Publisher's Note: The statements, opinions and data contained in all publications are solely those of the individual author(s) and contributor(s) and not of MDPI and/or the editor(s). MDPI and/or the editor(s) disclaim responsibility for any injury to people or property resulting from any ideas, methods, instructions or products referred to in the content.